AIP | Applied Physics Letters

Enhancement of light-extraction efficiency in AlGaInP light-emitting diodes using evanescent wave coupling effect

Guo-Dong Hao and Xue-Lun Wang

Citation: Applied Physics Letters **103**, 231112 (2013); doi: 10.1063/1.4842215
View online: http://dx.doi.org/10.1063/1.4842215
View Table of Contents: http://scitation.aip.org/content/aip/journal/apl/103/23?ver=pdfcov
Published by the AIP Publishing

Enhancement of light-extraction efficiency in AlGaInP light-emitting diodes using evanescent wave coupling effect

Guo-Dong Hao and Xue-Lun Wang
Nanosystem Research Institute, National Institute of Advanced Industrial Science and Technology (AIST), Tsukuba Central 2, Tsukuba 305-8568, Japan

(Received 12 September 2013; accepted 22 November 2013; published online 6 December 2013)

Sub-wavelength-sized ridge structures that satisfy evanescent wave coupling effect requirements at the emission wavelength were fabricated through the photolithography and wet chemical etching of the light-extraction surface of a thin-film type AlGaInP light-emitting diode (LED). By doing this, the light output power relative to a reference LED with a flat light-extraction surface was increased by a factor of approximately 3.8, corresponding to an equivalent enhancement in light-extraction efficiency that is possibly attributable to an evanescent wave coupling effect occurring on the surfaces of the minute ridge structures. © *2013 AIP Publishing LLC*.
[http://dx.doi.org/10.1063/1.4842215]

High-brightness light-emitting diodes (LEDs) have been widely used in commercial applications such as automotive lighting, full-color displays, and general illumination. Given the extensive investigations on the epitaxial qualities of AlGaInP materials in past years, the internal quantum efficiencies of AlGaInP-based red LEDs has reached near 100%;[1] however, their light-extraction efficiencies are still limited owing to the occurrence of strong total internal reflections at the air-semiconductor interface caused by the large refractive index differential between AlGaInP ($n \sim 3.3$) and air. In a conventional flat-surface LED, only the light within a narrow escape cone can be extracted into the air, and more than 90% of the light remains trapped within the device before finally being transformed into heat. To enhance the light-extraction efficiency of AlGaInP-based LEDs, therefore, several approaches have been proposed and demonstrated, including wafer bonding,[2] chip geometry shaping,[3] and random surface texturing.[4–6] One such method involves cutting a chip into a truncated-inverted-pyramid (TIP) structure[3] that can provide multiple escape routes by allowing light totally reflected at one facet to arrive at another facet at an incidence angle smaller than the critical angle for total internal reflection. Such structures have produced external quantum efficiencies (EQEs) as high as about 33% without encapsulation. Another widely employed architecture is the so-called thin-film LED, which has a randomly textured surface on the light-extraction side and a highly reflective metal mirror on the back side. In these structures, multiple reflections between the textured surface and the metal mirror, in which the propagation direction is randomized by the textured surface, allows totally reflected light to be redirected into an escape cone, enabling EQEs similar to those of TIP structures (about 40%) to be attained.[4] However, further improvements in light-extraction efficiency using conventional techniques such as these are likely to be very difficult, as extraction mechanisms based on multiple reflections must compete with absorption losses within the epitaxial layers and reflection losses at the interfaces. Another technique under extensive ongoing investigations with the potential for significantly increasing light-extraction efficiency involves the use of photonic crystals; however, as the highest EQE currently attainable by AlGaInP LEDs using photonic crystals is approximately 19%,[7] it remains difficult for photonic crystal techniques to compete with those using TIPs and thin-film techniques.

Previously, we proposed an effective light-extraction technique based on the evanescent wave coupling effect in a narrow ridge structure that is capable of directly extracting light outside of the escape cones into the air.[8] This effect is schematically illustrated in Fig. 1: when light emitted from the center of a quantum well (QW) located beneath the ridge structures arrives at the two side facets of the ridge at incidence angles comparable to or greater than the critical angle of total internal reflection, evanescent waves are generated at the two air-semiconductor sidewall interfaces. These evanescent waves then propagate along the interfaces towards the ridge top and are transformed into light propagating in air through coupling when they meet at the sub-wavelength-sized ridge top facet. Although photoluminescence studies have revealed significant enhancement of light-extraction efficiency in selectively-grown AlGaAs/GaAs and AlGaInP/GaInP ridge structures,[9–11] it is vital to implement this technique to a real LED device under current injection. In this paper, we report on the application of this technique to AlGaInP/GaInP LEDs and the resulting considerable enhancement in light-extraction efficiency in comparison with conventional techniques.

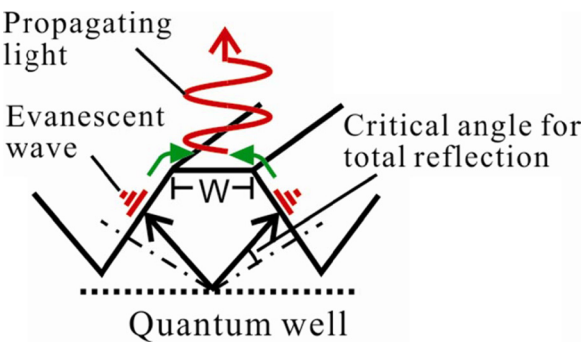

FIG. 1. Schematic illustration of the evanescent wave coupling effect occurring in a sub-wavelength-sized ridge structure.

Figure 2(a) shows a schematic cross-section of a fabricated AlGaInP LED with ridge structures on its light-extraction surface (R-LED). The original epitaxial structure was grown on a (001) GaAs substrate that was mis-oriented toward the [110] direction by 10° in order to suppress spontaneous ordering in the GaInP and AlGaInP epilayers deposited by metal organic vapor phase epitaxy (MOVPE).[12] Trimethylaluminum (TMAl), triethylgallium (TEGa), and trimethylindium (TMIn) were employed as group III source materials and tertiarybutylarsine (TBAs) and tertiarybutylphosphine (TBP) were employed as group V sources. Disilane (Si_2H_6) and dimethylzinc (DMZn) were used, respectively, as n- and p-type doping sources. The LED structure was composed of a 0.4 μm-thick n-$Al_{0.7}Ga_{0.3}As$ etch-stop layer, a 30 nm-thick Si-doped GaAs ohmic contact layer, a 0.8 μm-thick Si-doped $Al_{0.7}Ga_{0.3}As$ layer for forming ridges, a 2 μm-thick Si-doped $(Al_{0.7}Ga_{0.3})_{0.5}In_{0.5}P$ current-spreading layer, a 0.1 μm-thick undoped $(Al_{0.7}Ga_{0.3})_{0.5}In_{0.5}P$ cladding layer, a three-period $(Al_{0.5}Ga_{0.5})_{0.5}In_{0.5}P/Ga_{0.5}In_{0.5}P$ multiple QWs active layer (well thickness ~ 7 nm), a 0.2 μm thick undoped $(Al_{0.7}Ga_{0.3})_{0.5}In_{0.5}P$ cladding layer, a 2 μm-thick Zn-doped $(Al_{0.7}Ga_{0.3})_{0.5}In_{0.5}P$ cladding layer, and a 10 nm-thick heavily Zn-doped GaAs ohmic contact layer. The wafer was thermally annealed in N_2 at 500 °C for 2 min in order to activate its Zn acceptors. After the formation of a Ti/Pt/Au ohmic contact electrode in the form of an array of small circles (circle diameter ~ 1 μm, surface coverage ~ 1%) on the Zn-doped GaAs surface, a Ag layer was deposited onto the wafer surface by E-beam evaporation to serve as a reflective mirror, followed by the deposition of a diffusion barrier (Ti/Pt) for eutectic bonding. Next, AuSn eutectic bonding layer with a Au composition of 80 wt. % and a total thickness of 2 μm was prepared by alternative evaporation of Au and Sn layers onto the surfaces of the above LED wafer and an n-GaAs submount wafer on which AuGe/Ni/Au ohmic contact was already formed. The LED wafer was then flipped and attached to the GaAs submount by eutectic bonding which was carried out at a temperature of 380 °C and a pressure of 0.2 MPa. The original GaAs substrate was milled to about 50 μm by mechanical lapping and removed completely by selective chemical etching with a citric:H_2O_2 = 4:1 solution. Next, the exposed $Al_{0.7}Ga_{0.3}As$ etch stop layer was removed by immersing the sample into a HF:H_2O = 1:10 solution. Minute ridge structures with a 1.5 μm period were then fabricated through photolithography and wet chemical etching of the exposed 30-nm thick GaAs ohmic contact layer and the 0.8-μm thick underlying $Al_{0.7}Ga_{0.3}As$ layers. As shown in Figure 2(b), the lateral width of the top-flat facet and the depth of the ridge are about 0.38 and 0.6 μm, respectively; as confirmed by a finite-difference time-domain simulation (FDTD), these dimensions allow for the achievement of a strong evanescent wave coupling effect.[8–11] Finally, n- and p-electrode were formed on the ridge and GaAs submount surfaces through photolithography and E-beam evaporation, respectively. The p-electrode covered the entire back surface of the GaAs submount while the n-electrode (Pd/Ge/Au) was fabricated in the form of four whirlpool-shaped fingers with a 100 μm-diameter circle at their center to serve as the bonding pad, as shown in the inset of Fig. 3. The n-electrode covered about 4% of the total chip area, with each metal finger having a width of about 4.5 μm and a distance from its adjacent finger of 100 μm. The wafer was isolated into 1 × 1 mm^2 LED chips through chemical wet etching. Reference LEDs with flat-surfaces (F-LED) were also fabricated for the purpose of performance comparison, and in order to avoid any ambiguities owing to wafer non-uniformity, both the F- and R-LEDs were fabricated side-by-side from the same 12 × 13 mm^2 wafer.

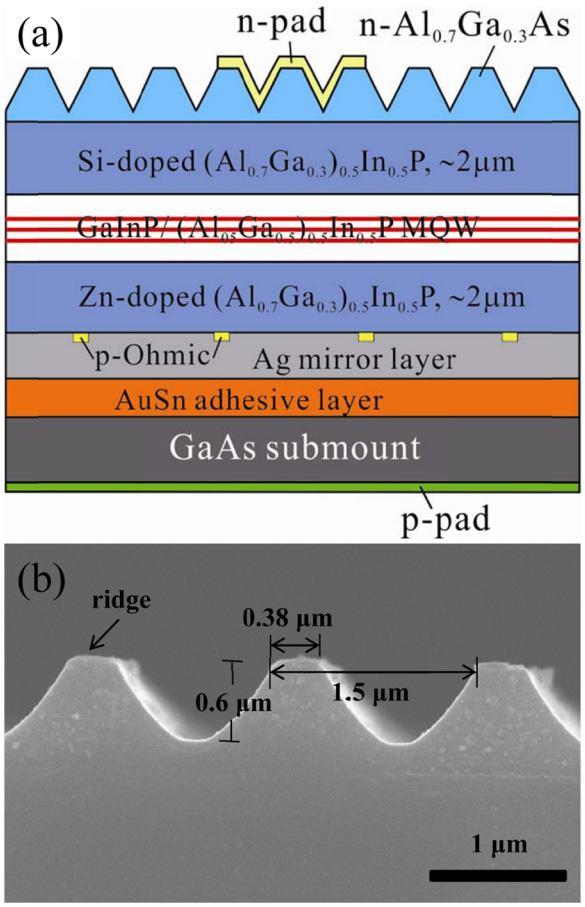

FIG. 2. (a) Schematic cross-section of an AlGaInP LED with sub-wavelength-sized ridge structure on the light-extraction surface. (b) Scanning electron microscope image of the ridge structure fabricated on the LED surface.

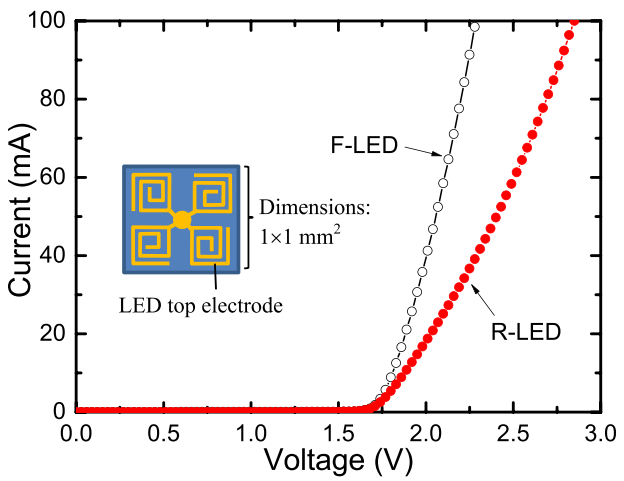

FIG. 3. Comparison of measured *I-V* characteristics of F- and R-LED. The inset shows a top view of the n-electrode.

Figure 3 shows a comparison of the current versus voltage (*I-V*) characteristics of the two types of chips. It is seen that while the turn-on voltages of the two LEDs are nearly identical, the R-LED has a slightly higher series resistance (about 9.0 Ω) than the F-LED (about 4.5 Ω), a discrepancy that can be attributed to the R-LED having an n-electrode ohmic contact area of about 1/4 that of the F-LED (see the discussion of Fig. 5 for further details) and a suboptimal ohmic contact resistance. Assuming that this difference in series resistance results primarily from the difference in contact resistance between the respective ohmic electrodes, the specific contact resistivity can be estimated to be about $6.0 \times 10^{-4}\,\Omega \cdot \mathrm{cm}^2$, which is about two orders of magnitude higher than the best value ($10^{-6}\,\Omega \cdot \mathrm{cm}^2$) obtained for Pd/Ge/Au ohmic material.[13,14] We are in the process of trying to reduce the contact resistance by optimizing the ohmic preparation process.

Figure 4 shows the typical light output power (measured by a Si photodiode from the top of the device using a probe measurement system) versus current (*L-I*) characteristics of the R- and F-LEDs. It is seen that at a lower injection current of about 5 mA, the R-LED has a light output power that is about 3.8 times (ridge to flat ratio in Fig. 4) higher than that of the F-LED. It is also apparent that this relative enhancement of light output power decreases with increasing injection current but remains as high as about 3 times at an injection current of 100 mA; the causes of this decrease will be discussed next. As these samples were fabricated side-by-side from the same 12×13 mm^2 sized wafer, all else being equal they would be expected to have similar internal quantum efficiencies; as such, the above results clearly indicate that the ridge structures in the R-LED sample are responsible for a 3.8-fold enhancement in light-extraction efficiency at lower injection currents. In AlGaInP-based LEDs, the light-extraction enhancement relative to planar-surface samples obtained by employing conventional techniques such as random surface roughening and photonic crystal use is typically in the range of 1.5–1.8,[4,15–17] which would imply that the evanescent wave coupling effect is indeed much more efficient than conventional techniques. This is because the underlying principle of conventional techniques including the TIP structure and thin-film LEDs is the redirection of totally reflected light into an escape cone through multiple reflections within the device; a conventional AlGaInP-based LED requires at least 10 reflection events for light generated in its active layer to escape to the air even with an ideal diffuse surface.[18] In the case of multiple reflections, any small absorption by the metal mirror and epilayers will cause considerable losses in light-extraction efficiency due to the large number of reflection events. In contrast, the proposed technique allows a large portion of the light from outside the escape cone to be directly extracted to the air through the evanescent wave coupling effect, which greatly reduces the number of reflection events needed for light extraction.

In order to clarify the mechanism underlying the decrease in ridge-to-flat enhancement ratio with increasing injection current, we performed a theoretical calculation of the current-spreading length. The current injected from the opaque metal electrode extends away from the metal contact region to the regions not covered by the electrode (current-spreading region) through n-type AlGaInP and AlGaAs current-spreading layers between the top electrode and the active layer. Only light generated in the current-spreading region has the opportunity to be extracted into the air, while any light generated beneath the opaque metal electrode will be reflected back to the device or absorbed by the electrode. The current-spreading length L_s is given by $L_s = \sqrt{\frac{t n_{ideal} kT}{\rho J_0 e}}$,[18] where t is the thickness of the current-spreading layer, n_{ideal} is the diode ideality factor (~1.4, as obtained from *I-V* measurement results), ρ is the bulk resistivity of the current-spreading layer (0.16 Ω·cm, as determined by Hall measurement), and J_0 is the current density beneath the

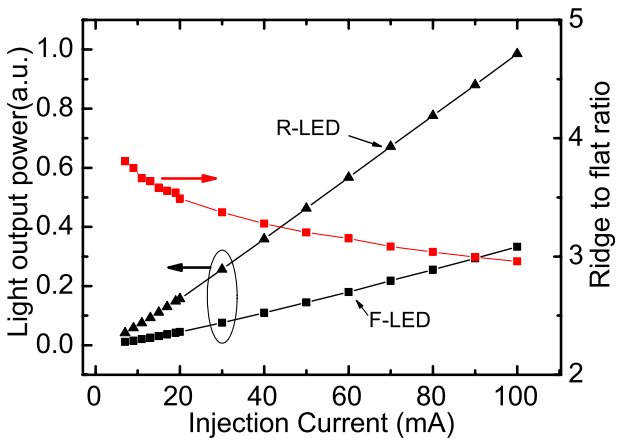

FIG. 4. Comparison of measured *L-I* characteristics of F- and R-LED and enhancement ratio of the light out power of an R-LED compared to an F-LED.

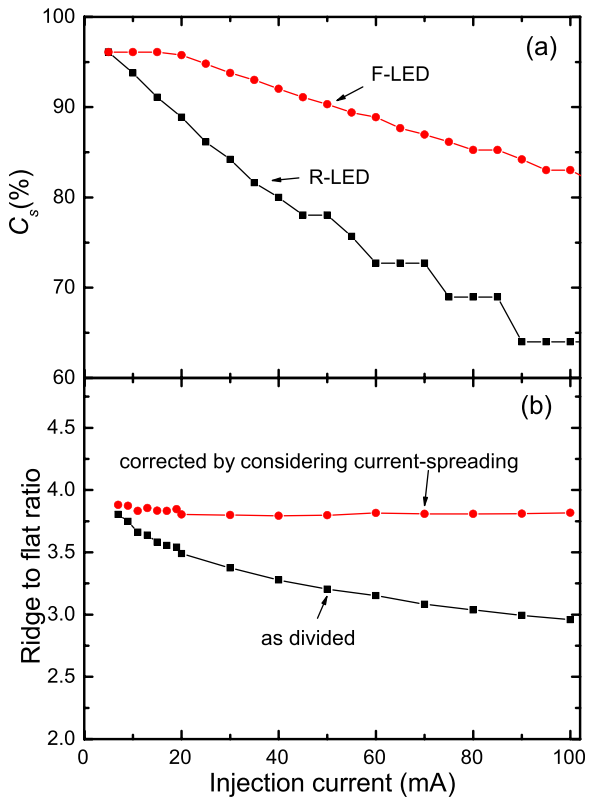

FIG. 5. (a) Current-spreading efficiency C_s versus injection currents for F- and R-LED. (b) Enhancement of the light out power of R-LED compared to F-LED taking into account the current-spreading.

metal electrode. The n-AlGaInP and n-AlGaAs current-spreading layers in the F-LED have thicknesses of 2.0 and 0.8 μm, respectively, while the average layer thickness of the n-AlGaAs layers in the R-LED is about 0.3 μm. In the R-LED, only the ridge-top facets at which the GaAs ohmic contact layer remains can form good ohmic contacts with the evaporated metal; as the ridge width is about 0.38 μm (corresponding to a ridge period of 1.5 μm), the total effective surface area is only about 1/4 that of the F-LED, resulting in an R-LED injection current density about 4 times that of the F-LED under an identical injection current. A top view of the n-electrode is illustrated in the inset of Fig. 3. In our calculations, the electrode was assumed to have a linear stripe geometry with a width of r_c.[18] We defined the current-spreading efficiency as $C_s = \frac{2L_s}{r_c+2L_s}$, which represents the ratio of current in the current-spreading region to the entire injection current. The spreading efficiency is given as a function of injection current in Fig. 5(a), from which it is seen that the C_s of F-LED reaches a maximum of about 96% (for ~4% of the surface covered by opaque electrode material) over a lower range of injection current of 5–20 mA, meaning that the current is sufficiently extended to the entire chip plane. With increasing injection current, the C_s of F-LED decreases slowly to ~83% at a current of 100 mA. The value of C_s in the R-LED decreases with increasing injection current at a much faster rate than in the F-LED; its value reaches as low as 64% at an injection current of 100 mA. By taking into account this current-spreading differential, the enhancement ratio of light-extraction efficiency as a function of injection current can be corrected, as shown in Fig. 5(b). It is seen that the corrected enhancement ratio has a nearly constant value of 3.8 over the entire injection current range of 5–100 mA.

In this study, a light-extraction technique based on the evanescent wave coupling effect in minute ridge structures was implemented in an AlGaInP-based red LED by forming ridge structures on the light-extraction surface of a thin-film type device. Using this ridge architecture, light-extraction efficiency was enhanced by a factor of 3.8 over that of a reference device with a flat light-extraction surface. We believe that our technique represents a significant step in the development of ultrahigh-efficiency LEDs.

[1]G. B. Stringfellow and M. G. Craford, *High Brightness Light Emitting Diodes* (Academic Press, Boston, 1997).
[2]F. A. Kish, F. M. Steranka, D. C. DeFevere, D. A. Vanderwater, K. G. Park, C. P. Kuo, T. D. Osentowski, M. J. Peanasky, J. G. Yu, R. M. Fletcher, D. A. Steigerwald, M. G. Craford, and V. M. Robbins, Appl. Phys. Lett. **64**, 2839 (1994).
[3]M. R. Krames, M. Ochiai-Holcomb, G. E. Hofler, C. C. Coman, E. I. Chen, I. H. Tan, P. Grillot, N. F. Gardner, H. C. Chui, J.-W. Huang, S. A. Stockman, F. A. Kish, M. G. Craford, T. S. Tan, C. P. Kocot, M. Hueschen, J. Posselt, B. Loh, G. Sasser, and D. Collins, Appl. Phys. Lett. **75**, 2365 (1999).
[4]R. Wirth, S. Illek, C. Karnutsch, I. Pietzonka, A. Plössl, P. Stauss, W. Stein, W. Wegleiter, R. Windisch, H. Zull, and K. Streubel, SPIE **4996**, 1 (2003).
[5]K. Streubel, N. Linder, R. Wirth, and A. Jaeger, IEEE J. Sel. Top. Quantum Electron. **8**, 321 (2002).
[6]R. Windisch, R. Butendeich, S. Illek, S. Kugler, R. Wirth, H. Zull, and K. Streubel, IEEE Photon. Technol. Lett. **19**, 774 (2007).
[7]K. Bergenek, C. Wiesmann, R. Wirth, L. O'Faolain, N. Linder, K. Streubel, and T. F. Krauss, Appl. Phys. Lett. **93**, 041105 (2008).
[8]X.-L. Wang and T. Takahashi, Jpn. J. Appl. Phys. **51**, 040205 (2012).
[9]G. D. Hao, J. Seo, and X.-L. Wang, Phys. Status Solidi C **9**, 306 (2012).
[10]X.-L. Wang, S. Furue, M. Ogura, V. Voliotis, M. Ravaro, A. Enderlin, and R. Grousson, Appl. Phys. Lett. **94**, 091102 (2009).
[11]G. D. Hao and X.-L. Wang, Appl. Phys. Lett. **100**, 091107 (2012).
[12]A. Gomyo, T. Suzuki, and S. Iijima, Phys. Rev. Lett. **60**, 2645 (1988).
[13]L. C. Wang, P. H. Hao, and B. J. Wu, Appl. Phys. Lett. **67**, 509 (1995).
[14]P. H. Hao, L. C. Wang, F. Deng, S. S. Lau, and J. Y. Cheng, J. Appl. Phys. **79**, 4211 (1996).
[15]S.-K. Kim, H. D. Song, H. S. Ee, H. M. Choi, H. K. Cho, Y. H. Lee, and H.-G. Park, Appl. Phys. Lett. **94**, 101102 (2009).
[16]Y. J. Lee, T. C. Lu, H. C. Kuo, S. C. Wang, T. C. Tsu, M. H. Hsieh, M. J. Jou, and B. J. Lee, Mater. Sci. Eng. B **138**, 157 (2007).
[17]R. H. Horng, T. M. Wu, and D.-S. Wuu, J. Electrochem. Soc. **155**, H710 (2008).
[18]E. F. Schubert, *Light Emitting Diodes* (Cambridge University Press, Cambridge, 2006), pp. 133, 187.